INTERNATIONAL JOURNAL OF AUTOMOTIVE AND MECHANICAL ENGINEERING
ISSN: 2229-8649 e-ISSN: 2180-1606
VOL. 21, ISSUE 2, 2024, 11398 – 11414
DOI: https://doi.org/10.15282/ijame.21.2.2024.17.0880

RESEARCH ARTICLE

Application of Passive Technique to Cocoa Beans Batch Dryer and Assessment of Thin Layer Models

S. Tepthanee[1], J. Taweekun[2] and P. Vessakosol[2]*

[1]Energy Technology Program, Faculty of Engineering, Prince of Songkla University, Hat Yai, Songkhla 90112, Thailand
[2]Department of Mechanical and Mechatronics Engineering, Faculty of Engineering, Prince of Songkla University, Hat Yai, Songkhla 90112, Thailand
Phone: +6674287416; Fax: +6674558830

ABSTRACT - The objective of this work was to develop a hot air production system using twisted tapes (TT) for the specific purpose of drying cocoa. The study also aimed to analyze the drying characteristics and kinetics of cocoa beans under the specific conditions that were investigated. TTs were inserted into the pipes of the shell and tube heat exchanger with multiple tube passes (STHEX). A modified rocket stove was used to burn biomass. Insertion levels of typical TT are 0%, 17.24%, 34.48%, and 60.63%, representing A (plain tube), B, C, and D, respectively.TT with a higher insertion level results in increased heat transfer. However, this also leads to an increase in pressure loss, which in turn affects the fan power consumption required to maintain the desired flow rate. The insertion level of D was the best in this work. It was used to produce a hot air supply to the drying room. After fermentation, the initial moisture content (MC) of 5 kilograms of the cocoa beans was 56.48% (wet basis; wb). The cocoa beans were dried in a drying room at an airflow rate of 4.5 m^3/min. The MC declined from 56.48% to 5.13% (wb) within 14 hours. The present study only detected a falling rate period in cocoa bean drying. The Overhult model is the most effective model for this drying process. It has the potential to serve as a useful tool for engineering applications.

ARTICLE HISTORY
Received : 20th Sept. 2023
Revised : 07th May 2024
Accepted : 08th June 2024
Published : 20th June 2024

KEYWORDS
Heat exchanger
Passive techniques
Twisted tape
Thin layer models
Cocoa beans

1.0 INTRODUCTION

Heat exchangers (HEX) are devices that cause convective heat transfer by working fluid inside pipes and are used in several industries, such as refrigeration, automotive, computer chips, solar heat collector systems [1], chemical engineering processes, heat recovery, and power plants [2], as well as residential areas [3], and the food industry [4]. Processes involving heating and cooling demand limitless energy. There is great concern about the efficiency of HEXs involved in the economic running of industries, saving costs and materials, and protecting the environment [5]. By improving heat transfer in HEXs, significant energy savings can be achieved [6]. Passive techniques are modifications of surfaces or geometry, such as treated surfaces [7], rough surfaces [8], displaced enhancement devices [3], additives to fluids such as nanofluids [1], and vortex generator devices [3, 4]. TT is a commonly employed technique for improving heat exchange. The TT inserts can increase heat transfer by blocking the flow and partitioning the flow [9–13]. The blockage causes an increased pressure loss but leads to the secondary flow because of the swirl flow or vortex inside HEX tubes, which creates fluid mixing, reduces the thickness of the boundary layer [14, 15], and increases residence time [5]. For this insertion, the increasing convective heat transfer coefficient can occur without increasing the size of HEXs [16], reducing the costs of material and manufacturing HEXs [4, 17]. HEXs are utilized in the drying procedures of agricultural products to produce hot air. The drying process involves direct heat transfer. Heat transfer enhancement reduces energy consumption and improves drying efficiency, resulting in high-quality products with low costs [18].

Cocoa, scientifically known as Theobroma cacao, is a highly significant cash crop in numerous countries [19, 20], including Thailand. Most farmers in the south of Thailand choose to grow more cocoa than rubber because rubber's price is low. Cocoa beans are in high demand due to their being a crucial raw material for many industries, such as chocolate, pharmaceuticals, beverages, cosmetics, and toiletry products [21]. The quality of cocoa products depends on two main processes: fermentation and drying. The fermentation results in the final products having a good flavor, aroma, and quality. Quick drying blocks the complete fermentation involved in drying because it reduces acetic acid products, which were evaporated during the drying process, obtained from the oxidation of ethanol by bacteria [22]. Excessive drying leads to weight loss and increasing energy costs. As a result, the drying process removes moisture from cocoa or agricultural products through vaporization in the form of gas, making them free of humidity [18]. For dried cocoa beans, the suitable MC is between 5% and 8% (wb) for safe storage [20], including saving packaging and transportation costs [18]. Typically, cocoa beans are dried by spreading them out in a thin layer and allowing them to be exposed to the air; therefore, trying to imitate a thin layer of drying is studied using various models. The experimental data on cocoa bean drying are fitted in thin-layer mathematical models. Assume that the cocoa bean can be approximated as spheres [22].

Simulation and modeling have many advantages for facilitating study. It is low-cost and less time-consuming to study, especially on a large scale and for long-term research. Research flexibility is the ease with which one can adjust various

*CORRESPONDING AUTHOR | P. Vessakosol | ✉ vpassakorn@eng.psu.ac.th

parameters and conditions, thereby conducting a wide range of research without limitations and generating valuable insights. They facilitate scale-up from laboratory to industry. Modeling and simulation can help optimize process design by predicting how changes in equipment size or operating conditions affect process performance.

This study focuses on developing hot air production systems that apply to the cocoa bean drying process. The STHEX is inserted with typical twisted tape (5-twist ratio) to improve heat transfer enhancement. Two rocket stoves are used instead of conventional combustion. Drying kinetics typically involves mathematical modeling of moisture removal rates. Choosing the most appropriate models to explain the drying process and predict the moisture ratio (MR) of cocoa beans drying using a developed hot air production system.

Table 1. The simulations of heat transfer in a tested pipe with TT inserts

Simulation of fluid flow pattern	Fluids	Twisted tapes (TT)	Outcomes	Researchers
Turbulence	Air	Spaced short length	The optimal design of spaced short length in a pipe with flow at a Reynolds number ranging from 10,000 to 20200 can be a reference for industrial applications.	Wang et al. [4]
Turbulence	Air	Two plain TT (twist ratio of 3.46 and 7.6)	It is determined that the TT offers a superior increase in heat transfer at comparatively lower Reynolds numbers and twist ratios.	Tusar et al. [5]
Laminar	Water	Elliptic-cut TT	The friction factor and heat transfer were higher in a tube with an elliptic cut (0.4 cm cut depth and 2.93 twist ratio) than in a tube with other types of TT and a plain tube for all Reynolds numbers.	Salman et al. [23]
Turbulence	Water	Twisted oval tube with different TT. - classic - triple channel - perforated TT - four-channel - ribbed TT - center cleared - five channel	The highest thermal enhancement criterion was achieved from a twisted tube with a center cleared TT. An augmentation in the number of TT channels and the interface area between the TT and fluid results in a decrease in the thermal enhancement criterion.	Yu et al. [6]
Laminar	Water	U-loop pipe with no insert, full length (FTT), and short length (STT)	Enhancing heat transfer is significant with inserts. Heat transfer was obtained from FTT more than from STT and without inserts.	Bhuyan et al. [11]

Table 2. The modeling of various agricultural products

Agricultural Products	Drying methods	Models	Outcomes	Researchers
Cocoa beans	Heated batch drier	- Henderson and Pabis - Lewis	The increased drying temperature leads to increased drying rates, so the drying process is faster than at low temperatures. There were good results with two thin layer models.	Ndukwu et al. [22]
Cocoa beans	- Open sun dryers (OSD) - Conventional greenhouse (CGHD) - Modified green house (MGHD)	- Lewis - Overhult - Henderson and Pabis - Page	The MGHD gave a higher temperature than CGHD and OSD 2 and 8º C, respectively. It took a shorter time to dry the cocoa bean, reaching an MC of 5-8%. The most suitable models for the three drying procedures are Page and Overhult.	Banboye et al. [24]
Bitter Leaf Slices and Red Pepper	Electric oven dryer	- Logarithmic - Newton - Henderson and Pabis - Page	Drying temperature affects drying time and drying rates. The Page model was recommended for drying bitter leaf slices and red pepper.	Agarry [25]
Strawberry	Halogen drying	- Two-term model - Logarithmic - Page - Midilli - Lewis	High drying temperatures had a direct impact on the drying rate and drying coefficient, which led to a short drying time.	Al-Hilphy et al. [26]

Table 2. (cont.)

Agricultural Products	Drying methods	Models	Outcomes	Researchers
Strawberry	Halogen drying	- Wang and Singh - Henderson and Pabis - Modified Page - Approximation of diffusion	The page model was recommended for strawberry drying at temperatures of 70º C and 80º C. The strawberry drying occurred only in the falling rate period.	Al-Hilphy et al. [26]
Green peas	Solar cabinet, solar dehydrator and open sun drying	- Two-term - Newton - Verma - Two-term exponential - Henderson and Pabis - Overhults, - Logarithmic - Wang and Singh - Page	For the green pea drying process, a falling rate period was noticed. The cabinet drying had a higher green peas quality and acceptability than solar dehydrator and open sun drying. The Logarithmic model was recommended for green pea drying.	Kumar et al. [27]
Cocoa beans	Natural and artificial drying	- Newton - Verma et al., - Logarithmic - Wang and Smith - Two-term model, - Diffusion approach - Midili-Kucuk - Page - New model - Henderson and Pabis	The novel model that mixed the Two-term and the Page models was the most effective in describing the drying behavior of both artificial and natural drying.	Hii et al. [28]
Small Cardamom	Hot air oven	- Two-term - Logistic - Newton - Modified Page - Page - Two-term exponential - Henderson and Pabis	Drying rates were high at first, but they reduced as the sample's MC dropped. The Logistic model was recommended for small cardamom drying. As the drying air temperature increased, the drying rate constant, k, showed a significant rise.	Mishra et al. [29]
Non-Fragrant and Fragrant Paddy	Circulating bed-type dryer	- Logarithmic - Verma et al. - Logistic - Page - Two-term exponential - Henderson and Pabis - Newton - Approximation of diffusion - Modified Page	The Approximation of the diffusion model had good results that fit the experimental data for both non-fragrant and fragrant paddy. The Logarithmic model also had good agreement with the results of non-fragrant paddy at a drying temperature of 45 ºC. The drying rate of paddy was dependent on grain size, relative humidity, and drying temperature.	Taveesuvun et al. [30]
Ginger rhizomes	ARS-680 environmental chamber	- Logarithmic - Newton - Midilli et al. - Modified Page - Verma et al. - Henderson and Pabis - Wang and Singh - Diffusion approach - Two-term - Modified Henderson and Pabis - Two-term exponential - Page	The higher drying temperature caused ginger shrinkage and surface discoloration. The two-term exponential model was recommended for ginger rhizome drying.	Gbasouzor et al. [31]
Jackfruit	Far-infrared (FIR) dryer	- Logarithmic - Newton - Wang and Singh - Page - Modified Page - Two-term exponential - Henderson and Pabis - Midilli et al.	Increased drying temperatures resulted in augmented drying rates, reduced drying times, and reduced energy consumption. The Page model was selected for jackfruit in the FIR dryer.	Praneetpolkrang and Sathapornprasath [32]

2.0 MATERIAL AND METHODS

The STHEX, as depicted in Figure 1, is placed inside a rectangular oven. Figure 6(b) illustrates the oven's insulation, which consists of brick and cement. The typical TT, having a twist ratio of 5, as depicted in Figures 2 and 3, are inserted into the tubes of the STHEX illustrated in Figure 8. The rocket stove is employed as a substitute for traditional combustion methods. In this study, two rocket stoves with fans produced the heat from fuel combustion, which fed 1.5 kg/h manually. There are three steps by which the heat from the rocket stove's combustion transfers to the hot air: (1) hot gas convection and high-temperature burner radiation transfer heat to the surface outside the HEX; (2) heat moves from the outside surface to the surface inside the HEX through conduction; and (3) the air receives heat from the inside surface through convection. Finally, the hot air enters the drying room and passes over the cocoa bean surfaces to remove water from them.

2.1 Hot Air Production

Components of a hot air production system include an STHEX, a blower, rocket stoves, and twisted tape. The blower was installed outside the oven, and others were installed inside the oven.

2.1.1 Heat exchanger

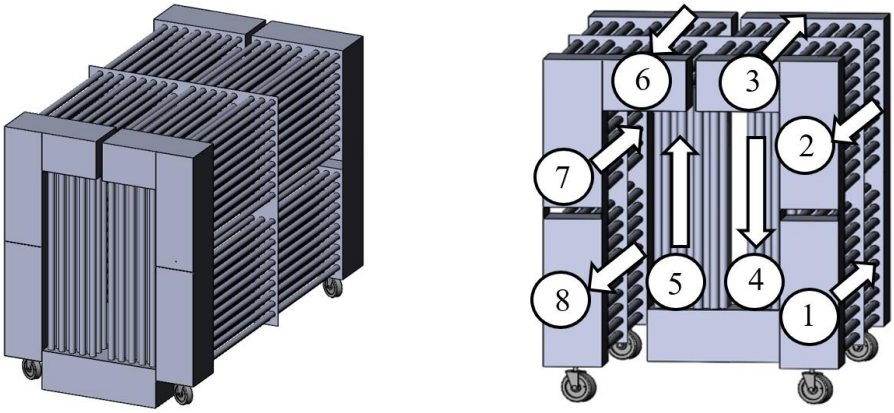

(a) (b)

Figure 1 Schematics diagram (a) Back of the STHEX (b) Fluid flow direction

Figure 1 shows the STHEX that were used in this experiment. The tubes were created using stainless steel. The dimensions of the STHEX are 0.8x1.5x1.2 m^3. The STHEX consists of 348 tubes, which are divided into eight distinct groups. Figure 1(a) displays a back view of the STHEX, while Figure 1(b) illustrates the directions of fluid flow. The air is introduced at inlet No. 1 and thereafter passes through Nos. 2, 3, 4, 5, 6, and 7 before finally exiting at outlet No. 8.

2.1.2 Twisted tape

Aluminum sheets measuring 0.9 mm in thickness were cut into segments of 20 mm in width and 122 mm in length. The cut pieces were twisted by the twist equipment. Figure 2 shows a typical TT with a twist ratio equal to 5. Figure 3 shows the twist ratio (y/W), where y is the 100-mm pitch and W is the 20-mm width, as well as the full length of TT insertion in the STHEX's tubes.

Figure 2. Typical twisted tape

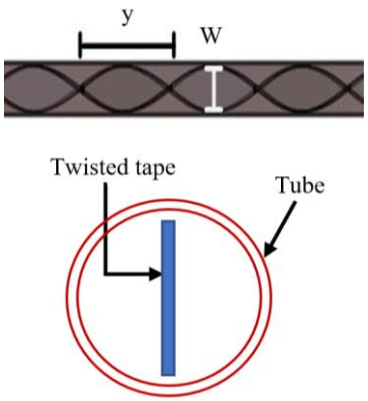

Figure 3. Insertion of twisted tape into a pipe

2.1.3 Modified rocket stove

Figure 4 depicts the biomass burner. The burner, also known as a modified rocket stove, was made of square steel tubes. The modified rocket stove has a fan and an ash channel for taking the ash out in front of the stove. The dimensions of a rocket stove are 7.62x27.94x65.24 cm^3.

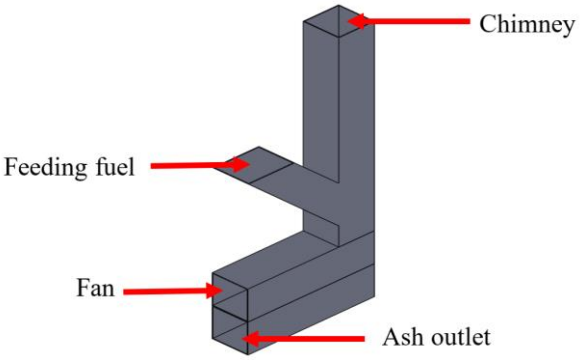

Figure 4. Schematic of a rocket stove

2.2 Drying Room

Figure 5(a) shows the drying room, which is made of aluminum sheets and insulated with synthetic rubber insulation on the walls. The dimension of the chamber is 1x1x1 m^3. Hot air from the STHEX enters the drying room at No.6 through distributed air tubes and exits at No.7. Grates-supported cocoa beans were placed on shelves at No.1, 2, 3, 4, and 5, as illustrated in Figure 5(b).

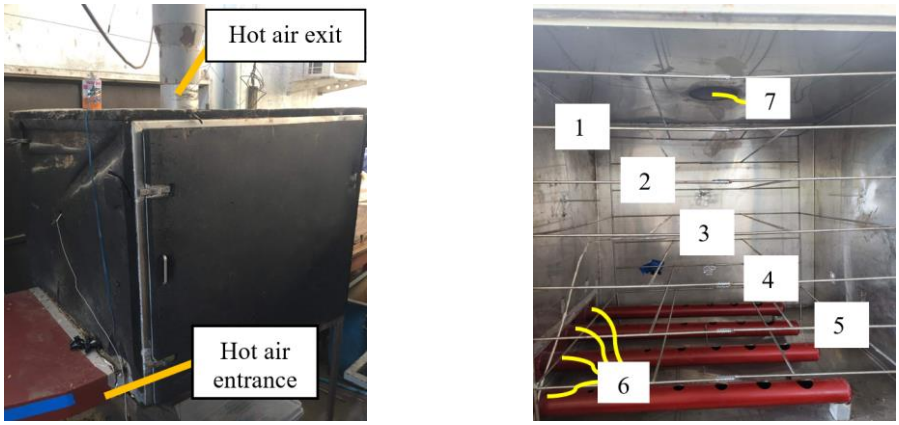

(a) (b)

Figure 5. Drying room (a) out of the chamber (b) inside of the chamber

2.3 *Experimental Setup*

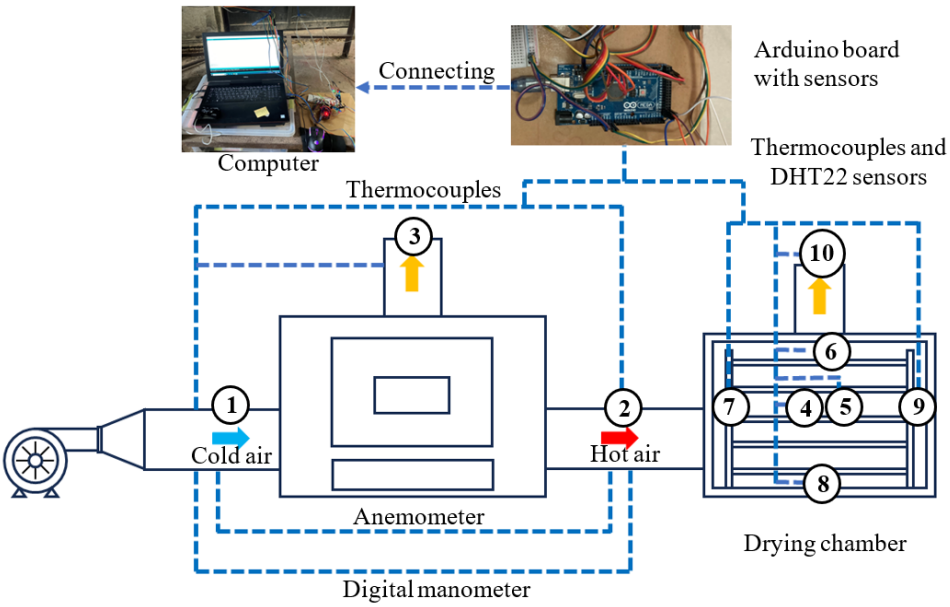

(a)

(b)

Figure 6. Experiment set up (a) diagram (b) connecting devices

Table 3. Listed of measurements

Instruments	Range	Accuracy
Digital manometer	±2.999 psi	±0.3%
Thermocouple Type K	0-600 ℃	±1.5 ℃
DHT22	RH: 0-100%	2-5%
	-40-80 ℃	±0.5 ℃
Digital weight	0-200 g	0.001 g
Anemometer	0.4-30.0 m/s	±2%

The experimental diagram for this present work is illustrated in Figure 6(a), and the connecting devices are shown in Figure 6(b) (Panorama view). The necessary facilities for conducting heat transfer tests include a 370-watt centrifugal blower, a measuring and recording apparatus, and test sections such as a HEX and drying room. The STHEX, depicted in Figure 1, was placed within a rectangular stove and covered with concrete insulation on the wall. The STHEX is linked to the drying room via the aluminum tube depicted in Figure 6. The details of measurement instruments are presented in Table 3.

The experimental setup follows three steps: At first, two rocket stoves were installed in the traditional stove (Figure 7(a)), which burned biomass fuel in the grate, whereas the air inlet was below the door of the STHEX. The biomass fuel is fed to the traditional stove, and the door of the stove can be opened at any time. The fuel can be fed through the opened door of the rocket stoves illustrated in Figure 7(b). During the second step of testing the STHEX, two thermocouples (type K) were employed to measure the air temperatures at the inlet (label No. 1) and outlet (label No. 2), as illustrated in Figure 6(a). The friction factor was determined by measuring the pressure loss using a digital manometer under isothermal

conditions without applying heat to the tube. The last step, the cocoa bean drying process, investigated water loss and drying rate throughout the process. The drying temperature was acquired using four K-type thermocouples at No. 5, 7, 8, and 9 (Figure 6) and two DHT22 sensors at No. 4 and 6 (Figure 6(a)). A DHT22 sensor was installed at the drying room exit at No. 10 (Figure 6(a)). All temperature and humidity data were collected by a data logger controlled by an Arduino Mega 2560 connected to an SD card module.

(a) (b)

Figure 7. Front of the stove (a) traditional stove (b) replacement with two rocket stoves

2.3.1 Hot air production setup

The STHEX has eight groups of tubes illustrated in Figure 1. Groups 1, 2, 7, and 8 have 60 tubes, and groups 3, 4, 5, and 6 have 27 tubes illustrated in Figure 8. There is a total of 348 pipes. The installation of twisted tapes in all pipes is guaranteed to be 100%. The case of twisted tape insertion is divided into 4 cases as follows:

In case A, the air flows through the plain tube without any inserts.

- In case B, 60 tubes were inserted in Group 1 (17.24% inserted).
- In case C, 120 tubes were inserted in groups 1 and 2 (34.48% inserted).
- In case D, 211 tubes were inserted in groups 1, 2, 3, and 6 for all, and in group 7 as 37 tubes (60.63% inserted).

The insertion ratio was determined by the group of tubes. The fluids flow more easily in a plain channel than in a channel with blockage. This is a reason to insert twisted tape into all tubes in each group in cases 1 and 2. In case 3, due to the restricted quantity of twisted tapes, it is not possible to insert them into all of the tubes in group 7. This is the maximum insertion ratio that can be provided.

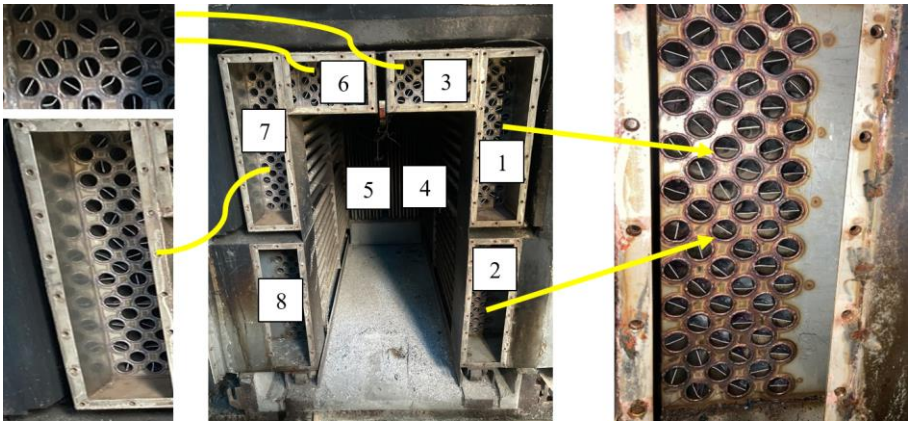

Figure 8. Twisted tape insertion in tubes (Case 4)

2.3.2 Drying process setup

The material for the experiments consisted of ripe fruits obtained from a local cocoa shop in Phatthalung province, Thailand. The fruits were opened (Figure 9(a)), and the selected seeds were collected in the basket. The seeds in the basket were fermented by covering them with fresh banana leaves (6-7 days duration), illustrated in Figure 9 (b) [20, 33] and were turned over every 24 h. After fermentation, the beans were washed in water, resulting in pulp being left [20, 34].

A total of 5 kilograms of cocoa beans were stored on the shelves in the drying room, as illustrated in Figure 9(c) and connected to a STHEX with twisted tape insertion in case of the best thermal efficiency. Heat sources are obtained from the combustion of biomass fuels.

(a) (b) (c)

Figure 9. Preparing cocoa (a) cut ripe cocoa (b) fermented cocoa beans (c) five shelves of cocoa beans

2.4 Methods

2.4.1 Thermal efficiency

Thermal efficiency is established as heat that HEX transfers to the air divided by heat from biomass combustion. It can be represented by the following Equation 1 [35]:

$$\eta_{th} = \frac{\dot{m}_a c_p \Delta T}{\dot{m}_f LHV_{fuel}} \tag{1}$$

where $\dot{m}_a$ and $\dot{m}_f$ are mass flow rate of air and fuel; c_p and LHV_{fuel} are specific heat capacity of air and low heating value of fuel, respectively. The LHV of wood is 18,648 kJ/kg [36].

2.4.2 Friction factor

The pressure loss (ΔP) is directly measured by a digital manometer. The friction factor (f) [15] is acquired by the following Equation 2:

$$f = \frac{\Delta P}{(L/D)(\rho U^2/2)} \tag{2}$$

The friction factor enhancement index [15] is calculated by the following Equation 3:

$$F = \frac{f}{f_p} \tag{3}$$

where f and f_p are the friction factors of tubes with inserts and plain tubes, respectively.

2.4.3 Moisture content

The MC of the cocoa beans is measured by fermented cocoa beans, both dried and undried. The samples in moisture boxes are placed in an electric oven at 105 °C till their weight remains constant [37]. On a digital weighing machine, both the sample's weights and the boxes for initial and final moisture are measured. The MC (%wb) is calculated [34] according to the following Equation 4:

$$\%\ \text{MC (wb)} = \frac{w_2 - w_3}{w_2 - w_1} \times 100 \tag{4}$$

where the w_1, w_2 and w_3 are the weight of the empty box, the weight of the box and moist samples, and the weight of the box and dried samples, respectively.

2.4.4 Moisture ratio

The variations of the cocoa beans MR with time were analyzed using experimental data. The MR is a representation of the amount of moisture remaining in the cocoa beans from the initial MC. The MR was determined using Equation 5 [25].

$$MR = \frac{M - M_e}{M_0 - M_e} \tag{5}$$

where M_0, M_e, and M represent the initial MC, the equilibrium MC, and the MC at time t, respectively. The equilibrium MC of samples was assumed to be zero[25] due to the small value of M_e, as compared to M and M_0 [38]. Calculation of the MR using Equation 6 follows:

$$MR = \frac{M}{M_0} \tag{6}$$

The MRs at time t for each cocoa bean sample were utilized to create drying curves, which were then compared to drying equations that predicted the MRs based on the thin layer model of drying, specifically the empirical and semi-theoretical approaches [38]. Empirical models were built from experimental data and dimensionless analysis [38] involving the relationship between MC and drying time. Nevertheless, there is no physical meaning to these model parameters [28, 38]. Typically, semi-theoretical models were rather simple to use and easy to adapt to data on food material drying [38]. The time requirement is decreased, and the semi-theoretical models do not consider the geometry of the dried material [38]. Eight drying models from Table 4 were used to fit the drying curves. The models were previously employed for diverse agricultural products such as cocoa, red pepper/blanched bitter leaf slices, strawberries, blanched green peas, and paddy [22, 24–30]. The models, based on experimental data, provide practical predictions of drying behavior, facilitating process control and optimization.

Table 4. Thin layer drying models are employed for fitting experimental data

Models	Equations	References
Newton/Lewis	MR=exp(-kt)	[22, 24, 38]
Page	MR=exp(-kt^n)	[22, 25, 26]
Verma	MR=a exp(-kt)+(1-a)exp(-gt)	[28]
Overhult	MR=exp((-kt)^n)	[24, 26, 27]
Wang and Singh	MR=1+at+bt^2	[26, 28]
Logarithmic	MR=a exp(-kt)+c	[25, 28]
Logistic	MR=a/(1+b exp(kt))	[29, 30]
Henderson and Pabis	MR=a exp(-kt)	[24, 25, 28]

k drying constant; t, drying time; a, c, n, g empirical:

The models were examined to understand the drying characteristics in terms of MR and drying rate. The MC is plotted with drying time, and its trend is used to choose the equation to fit the drying models. Nonlinear regression is commonly employed for simulating drying processes because the relationships between variables such as MC, drying time, temperature, and airflow rate are not linear [25, 27, 29]. Nonlinear regression analysis was conducted using the MATLAB commercial software (version R2023a) [25, 29]. The differences between predicted MR and experimental MR were determined in terms of statistical parameters. In terms of the quality of the best thin layer model, the coefficient of determination (R^2) [22, 25, 26, 29] value should be high, the root mean square error (RMSE) [24–26] given in Equation 7, the reduced chi-square ($\chi 2$) [22, 24, 28] given in Equation 8, and the standard error of estimate (SEE) [31] given in Equation 9 should be low [25, 28, 39].

$$RMSE = [\frac{1}{N}\sum_{i=1}^{N}(MR_{pre,i} - MR_{exp,i})^2]^{\frac{1}{2}} \tag{7}$$

$$\chi^2 = \frac{\sum_{i=1}^{N}(MR_{exp,i} - MR_{pre,i})^2}{N - z} \tag{8}$$

$$SEE = \frac{\sum_{i=1}^{N}(MR_{exp,i} - MR_{pre,i})^2}{z} \tag{9}$$

where $MR_{exp,i}$, $MR_{pre,i}$, N and z are the experimental MR, the predicted MR at ith data, the total number of observations and the total degrees of freedom of the regression model, respectively.

2.4.5 Drying rate (DR)

The drying rate (DR) at one moment in time is computed by following Equation 10:

$$DR = \frac{M_t - M_{t+\Delta t}}{\Delta t} \tag{10}$$

where M_t, $M_{t+\Delta t}$ and Δt are MC (%MC dry basis) at time t, MC (%MC db) at time $t + \Delta t$ and change in time, respectively.

The overall drying rate ($DR_{overall}$) is defined by the ratio of the difference between final moisture and initial content with total drying time defined as the following Equation 11:

$$DR_{overall} = \frac{M_f - M_i}{T} \tag{11}$$

where M_i, M_f and T are initial MC, final MC (g) and drying time (h), respectively.

3.0 RESULT AND DISCUSSION

3.1 Hot Air Production System

3.1.1 Replacement of conventional combustion with two rocket stoves

Figure 10 shows outlet exhaust gas. A traditional stove with ignition on the grate is illustrated in Figure 7(a) and has inlet air at the bottom of the door. At the first ignition, it is necessary to open the door for the entrance air to be sufficient in the combustion chamber to prevent the fire from dying out. About 10 minutes after fuel ignition, the door can be closed, but fuel feeding needed to open the door at any time resulted in heat loss in this case. In the case of rocket stoves, DC fans were installed in the inlet air of the rocket stoves (Figure 7(b)). The inlet air at the bottom was closed, as illustrated in Figure 7(b) at No. 2. Fuel is fed through a hole in a door illustrated in Figure 7(b) at No. 1, whereas the door is not opened. Adding two modified rocket stoves to traditional combustion resulted in more complete combustion. Smoke is one of their observations on complete combustion. Figures 10(a) and 10(b) indicate that incomplete combustion produces visible smoke, whereas complete combustion hardly produces it.

(a) (b)

Figure 10. Outlet exhaust gas (a) traditional stove (b) replacing with two rocket stoves

3.1.2 Thermal efficiency

Thermal efficiency of hot air production systems, which was calculated following Equation 1. Thermal efficiency was investigated in four STHEX cases, such as plain tubes (A) and three levels of twisted tape inserts. The levels of insertion of total tubes such as B, C, and D are 17.24%, 34.48%, and 60.63%, respectively.

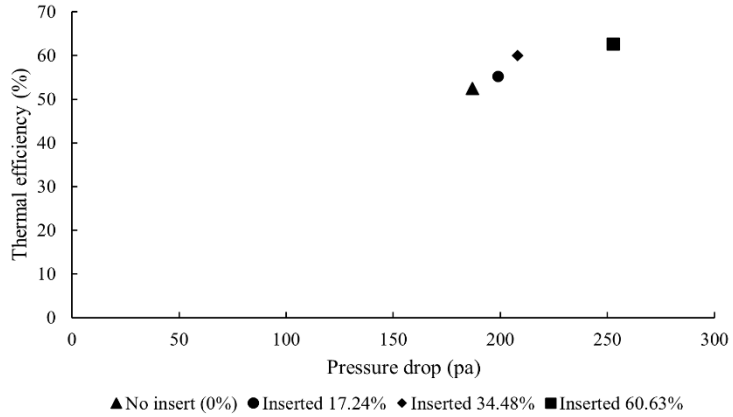

Figure 11. Thermal efficiency of hot air production system

Figure 11 shows the thermal efficiency of hot air production systems and pressure loss. For the plain tube (A) STHEX, the thermal efficiency is 52.47%. The thermal efficiencies of insertion levels B, C, and D are 55.17%, 60.00%, and 62.46%, respectively. The thermal efficiency rises with the increasing insertion ratio of TT, including pressure loss. The thermal efficiency and pressure loss tend to increase with the insertion level. The plain tube (A) and insertion levels B and C exhibit comparable patterns in terms of enhanced efficiency and negligible pressure loss rise. However, insertion level D shows a relatively minor improvement in thermal efficiency but a large increase in pressure loss compared to the other levels. It is necessary to optimize between enhanced heat transfer and pressure loss.

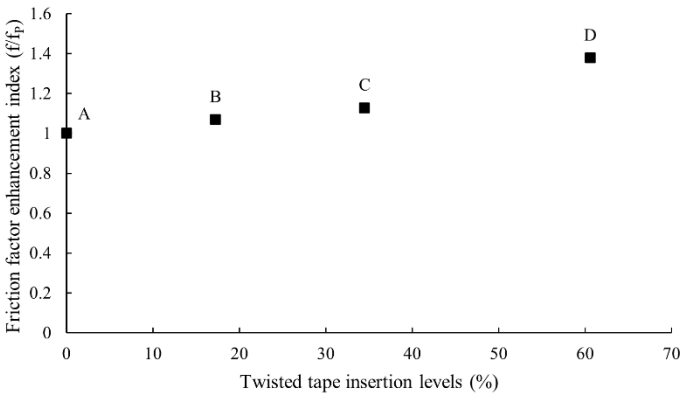

Figure 12. Friction factor enhancement index

The friction factor enhancement index (Figure 12) increases with increasing levels of insertion. At the levels of insertion such as A (plain tube) B, C, and D, the friction factor enhancement index of A, B, C, and D are 1, 1.07, 1.13, and 1.38, respectively.

60.63% of all tubes inserted with twisted tape, yielding the highest thermal efficiency, were used in the cocoa drying process. Insertion of twisted tape produces a swirl flow or vortex inside tubes, disrupting the thermal boundary layer, increasing residence time and fluid mixing [5], resulting in increased thermal efficiency with an increasing pressure loss[1, 15] at the same pumping power. Airflow encountering the twisted tapes caused increased resistance, which in turn led to a greater pressure loss. The trade-off is that it takes more fan power to maintain the flow rate. The fan consumes more power, leading to higher energy consumption and higher operation costs in the drying system. However, the TT enhances heat transfer and turbulence in the hot air that flows to the drying room. This advantage can improve drying rates, reduce drying time, and improve overall efficiency. The net impact on the system depends on the balanced benefits of enhanced heat transfer and penalty pressure loss.

3.2 Drying Process

3.2.1 Moisture content

MC (%wb) of dried cocoa beans in a drying room is illustrated in Figure 13 with hot air from a STHEX with twisted tape inserts. The D case (60.63% of total tubes) has the highest thermal efficiency in terms of a higher hot air temperature. Higher drying temperatures affect increased drying rates and reduced drying time. Gradually, the MC decreases with drying time. 56.48% (wb) of initial MC decreases to 5.13% (wb) when the drying time is 14 h. During the first hour to 4 hours, the MC rapidly decreases. After 5 hours, the MC gradually decreases throughout the drying periods.

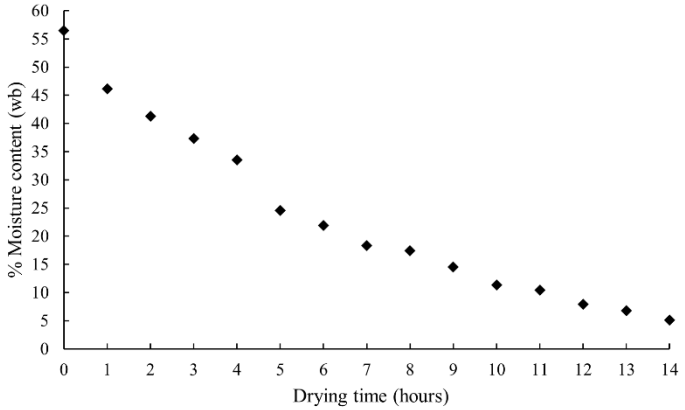

Figure 13. Variations in MC through drying time

In this drying system, the stove is not preheated, as illustrated in Figure 14. The temperature in the drying room gradually increases because of the use of the rocket stove with an adapted fuel feed rate. Surely, the temperature is not too high for drying cocoa. The cocoa bean can be put in the drying room before the STHEX starts to work. This step can reduce the fuel used to preheat the stove and save the system operating time.

3.2.2 Moisture ratio

Figure 14 shows the MR reduction (based on a dry basis) with drying temperature throughout the drying period. The cocoa beans were collected on shelves in a drying room at initial ignition to decrease heat loss from heating the oven. The biomass combustion was burned using two rocket stoves, replacing the traditional stove. In this system, 4.5 m^3/min of

airflow rate and a fuel feeding rate of 1.5 kg/h can gradually increase the drying temperature without overcooking caused by the initial heating oven.

In the continuous drying process, the drying temperature reaches 40-60°C for the first 1-4 hours, and the MR rapidly decreases from 0.66 to 0.39. Then, the MR gradually decreases from 0.39 to 0.09 during the drying period of 4-11 hours, with the drying temperature remaining stable at 55-60°C. After 11 hours of drying, the drying temperature gradually increases due to heat accumulation inside the furnace and drying room. However, the final temperature is 60-70°C during the 14-hour drying period, and the final MR is 0.04. The fuel feed rate is workable for feeding two rocket stoves in this study. The decreasing fuel feed rate below 1.5 kg/h causes fire extinguishing due to insufficient fuel to feed each hour. Therefore, controlling temperature is very difficult due to the abovementioned factors. In this experiment, the effect of temperature has not been studied yet.

In this experiment, MC is evaluated every hour as a hot air dryer. The MR of MC at the time per initial MC. The MR decreases as drying time increases. Comparing the MR of a hot air dryer in this experiment with a solar cabinet dryer [34] illustrated in Figure 15, the MR of a hot air dryer and solar cabinet has a similar trend. In this experiment, the MR in the first hour rapidly decreases. After 2 hours, the MR gradually decreases until 4 hours. During 4-6 hours, the MR rapidly decreases, and then the MR gradually decreases throughout drying periods, the same as Guda et al. [34]. The decreasing MR is exponential with time, which was revealed for many agricultural products [40]. Also, the exponential decrement of the MR can be explained by several thin-layer models.

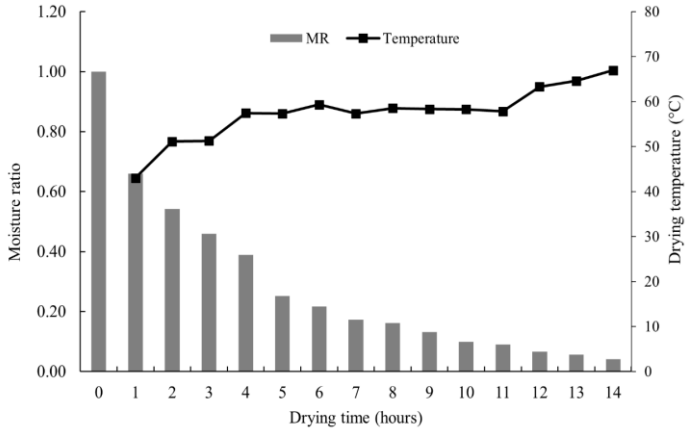

Figure 14. Variations of MR with drying time and drying temperature

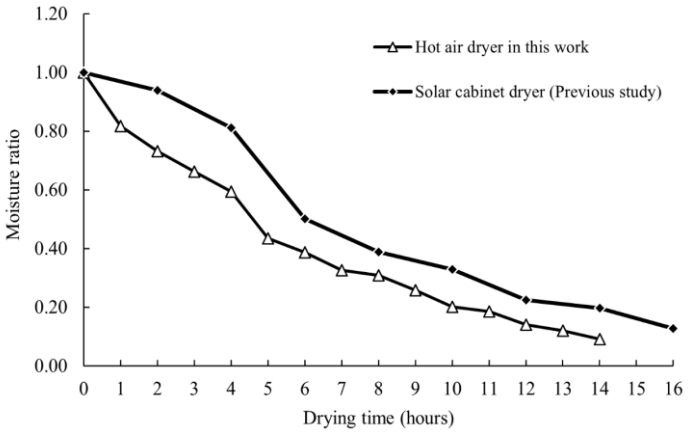

Figure 15. Comparison of MR in this study with the previous study [34]

3.2.3 Drying kinetics models

The variations of MC (%db) with time were changed into the MR and evaluated for eight different drying models as presented in Table 4. The results in Table 5 show the R^2, RMSE, and $\chi 2$ values were higher than 0.90, indicating a good fit [37]. For all models, the range of R^2, RMSE, $\chi 2$, and SEE values are 0.9172 -0.9885, 0.0502-0.1346, 0.0016-0.0133, and 0.0112-0.0533, respectively. From Table 5, considering the Newton model and the Overhult model, the R^2, RMSE, $\chi 2$ and SEE values of Newton and Overhult models are 0.9784 and 0.9885, 0.0688 and 0.0502, 0.0016 and 0.0017 and 0.0226 and 0.0112, respectively. The lowest of SEE and RMSE and the highest of R^2 are obtained from the Overhult model, but the lowest of $\chi 2$ is acquired from the Newton model because of the least number of prediction parameters. Because of the low value of R2 and the high values of SEE and RMSE, the Newton model was not suitable for use in this work. Thus, the Overhult model may be proposed as a suitable model to present the thin layer drying behavior of cocoa beans [24]. The best simulation model allows for the optimization of drying processes by accurately predicting the effects

of various parameters, such as airflow rate, temperature and material properties, on drying kinetics. By controlling drying parameters within specified ranges, the model can maintain product quality and consistency, reducing the over-drying or under-drying of products. By accurately predicting drying time and resource demands, it is possible to limit waste and avoid wasteful consumption, resulting in cost reductions and environmental advantages. Figure 16(a–h) shows a comparison graph between the predicted MR and experimental MR for the eight thin layer drying models in this work. The parameters k, n, a, c, and g were substituted in different models. Then, the predicted MRs were calculated, and graphs were plotted in Excel.

Table 5. Summaries of goodness fitting statistics of different models

Model	Statistical parameters				Coefficients and constants
	R^2	RMSE	$\chi 2$	SEE	
Newton	0.9784	0.0688	0.0016	0.0226	k=0.2617
Overhult	0.9885	0.0502	0.0017	0.0112	k=0.3221, n=0.7977
Page	0.9878	0.0518	0.0021	0.0138	k=0.4060, n=0.8038
Logarithmic	0.9864	0.0546	0.0036	0.0144	k=0.2791, a=0.9099, c=-0.0018
Henderson and Pabis	0.9874	0.0525	0.0033	0.0214	k=0.2807, a=0.9086
Logistic	0.9634	0.0896	0.0133	0.0533	k=0.5146, a=1.0252, b=0.5099
Wang and Singh	0.9172	0.1346	0.0061	0.0398	a=-0.1801, b=0.0084
Verma	0.9854	0.0566	0.0109	0.0438	k=0.3296, a=0.7085, g=0.3117

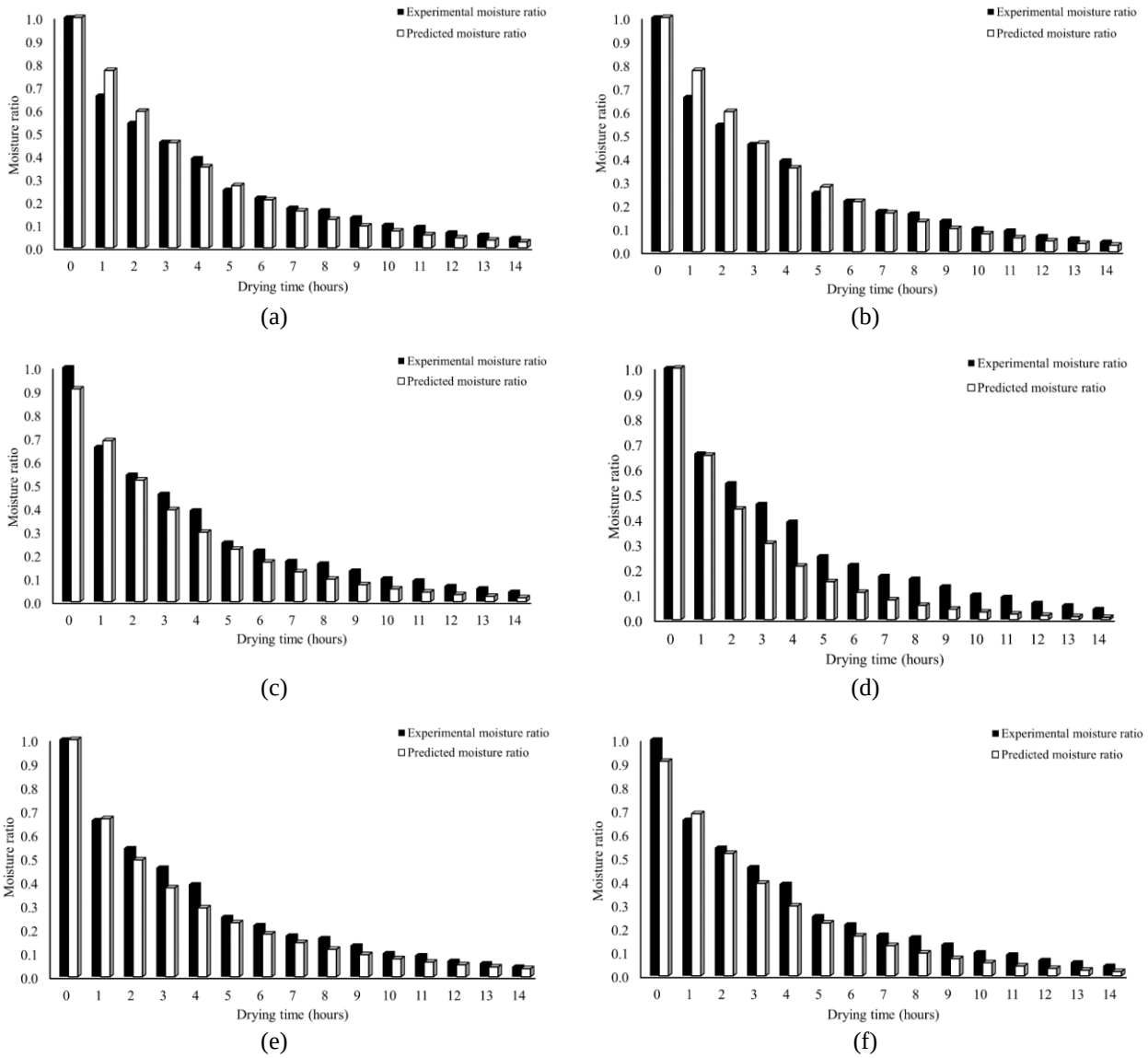

Figure 16. Representations of experimental MR versus predicted MR of cocoa beans for different thin layer drying models (a) Newton (b) Overhult (c) Logarithmic (d) Verma (e) Page (f) Henderson and Pabis

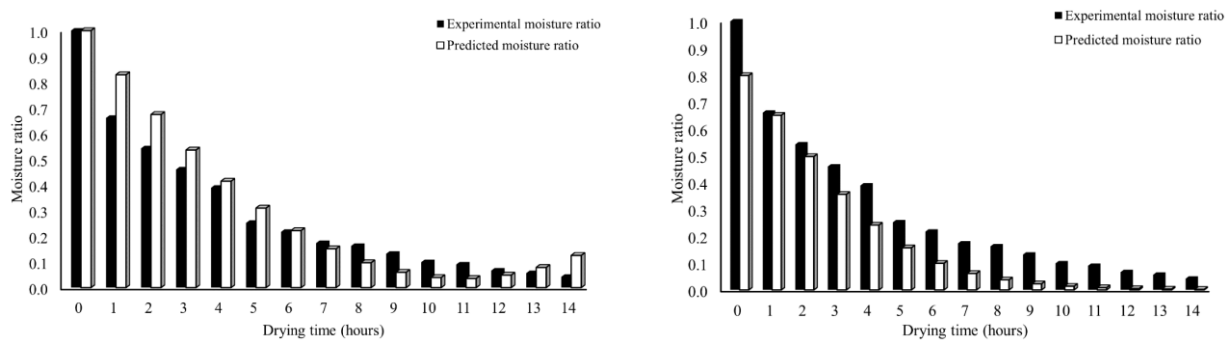

(g) (h)

Figure 16. (cont.) (g) Wang and Singh and (h) Logistic

3.2.4 Drying rate

Figure 17 illustrates the drying rates during the cocoa drying period. The drying rate is high during the initial drying period before rapidly decreasing over time [24]. For pre-drying treatment, such as the fermentation of a cocoa product, causing the loss of moisture. Therefore, the drying rate of cocoa after fermentation showed only a falling rate, which was observed for most agricultural products [24]. The drying rate ranged from 0.012 to 0.442 grams of water per gram of dry materials per hour. The variations in drying rate were not regular because of fluctuating temperature conditions. These can be described by an equation of the form:

$$\frac{dX}{dt} = aX^n \tag{12}$$

where $\frac{dX}{dt}$ and X are the drying rate and MC. The values of a and n are constants. The regression analysis results: a, n and R^2 are illustrated in Table 6.

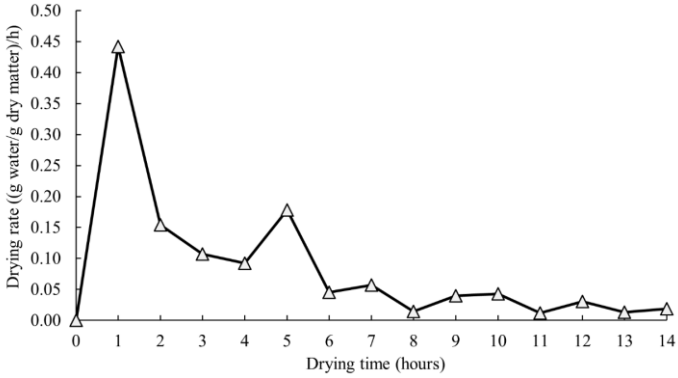

Figure 17. Drying rate through drying time

Table 6. Results of drying rate curves from regression analysis

	a	N	R^2
Hot air dryer	0.2716	1.5093	0.8236

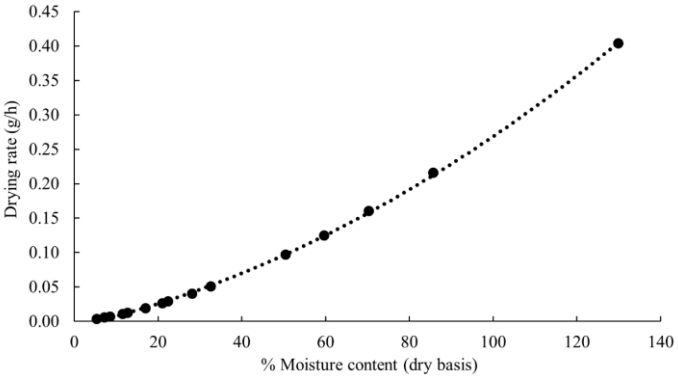

Figure 18. The variations of drying rate for cocoa bean drying

Figure 18 displays curves of cocoa bean drying plotted by the following Equation 12. The constants a and n are illustrated in Table 6. The R^2 is 0.8236. The curves of drying rate tend to decrease with a decrease in MC (% dry basis), conforming to Banboye et al. [24].

Equation 11 determines the overall drying rate. The experiment demonstrates that the hot air dryer in this study has an overall drying rate of 3.67 g/h, while the greenhouse dryer (MGHD) [24] and solar cabinet [34] are 1.21 g/h and 3.2 g/h, respectively. The existing hot air dryer can reduce cocoa beans' MC from 56.48% to 5.13% (wb) in 14 hours through continuous drying. The solar cabinet required 16 hours to decrease the MC from 49.88% to 6.36% (wb), while the MGHD needed four days to decrease the MC from 49.42% to 5.95% (wb). The current hot air dryer requires less time to dry cocoa beans to the expected MC. Because of the quick drying time, energy was conserved.

The drying process with hot air through the HEX entails the application of forced convective heat transfer, which requires the utilization of a fan to circulate the air. Biomass combustion supplied thermal energy to the hot air within the drying system. Short drying times can reduce fan power consumption and biomass combustion. Biomass is derived from the byproducts of agricultural products and the furniture manufacturing industry. The use of biomass as a fuel in the drying process has the advantage of reducing demand for fossil fuels and increasing waste disposal. Biomass possesses greater potential than fossil fuels in terms of its limitless amount and ability to emit less harmful greenhouse gases, such as carbon dioxide (CO_2). Although biomass combustion emits less CO_2 than fossil combustion, burning biomass still releases carbon dioxide. After harvesting, the drying process uses energy to dry agricultural products. There are numerous energy resources available for processes such as sunlight and biomass combustion. Environmental concerns about carbon dioxide-induced air pollution are widespread. CO_2 directly affects organisms, such as human and animal breathing. The combined drying methods between solar and hot air dryers are the guiding principle for reducing CO_2 emissions from biomass combustion and increasing solar drying efficiency. A concept of a combined dryer between a hot air dryer and a solar dryer to support the drying process. The hot air dryer can help increase the drying temperature in the solar dryer, reaching the expected temperature on days when the sky is dark or the light intensity is low.

4.0 CONCLUSION

The STHEX was inserted by twisted tapes into its tubes at varying insertion levels. The insertion levels A (plain tube), B, C, and D are 0%, 17.24%, 34.48%, and 60.63%, respectively. The insertion level of D was the best in this work. The authors recommended it for a small batch of cocoa bean drying. The drying rates were also reported. The MR was fitted in eight thin-layer modes to select the best model. The findings of the study are:

- The thermal efficiencies of insertion levels A, B, C, and D are 52.47%, 55.17%, 60.00%, and 62.46%, respectively.
- Twisted tape with a higher level of insertion exhibits better heat transfer, resulting in an increase in pressure loss.
- The hot air dryer that was developed in this study can decrease MC from 56.48% to 5.13% (wb) within 14 hours.
- In the current investigation, there is no period of constant drying rate; instead, cocoa beans were dried during a falling rate period.
- The best drying model for cocoa beans is the Overhult model, and this has the potential to serve as a useful tool for engineering applications.

In the future, the twisted tape can be adapted to the process of drying other agricultural materials. This machine can scale-up to industrial production.

5.0 ACKNOWLEDGEMENT

The authors acknowledge thanks to the Department of Chemical Engineering, and especially the Department of Mechanical and Mechatronics Engineering for their assistance in conducting measurements and providing laboratory facilities. The Engineering Graduate Scholarship, Faculty of Engineering, and Graduate Study Research Grant at Prince of Songkhla University have provided support for the research.

6.0 REFERENCES

[1] S. Ahmad, S. Abdullah, and K. Sopian, "A review on the thermal performance of nanofluid inside circular tube with twisted tape inserts," *Advances in Mechanical Engineering*, vol. 12, no. 6, pp. 1–26, 2020.

[2] S. Chokphoemphun, M. Pimsarn, C. Thianpong and P. Promvonge, "Thermal performance of tubular heat exchanger with multiple twisted-tape inserts," *Chinese Journal of Chemical Engineering*, vol. 23, pp. 755–762, 2015.

[3] A. Hasanpour, M. Farhadi, and K. Sedighi, "A review study on twisted tape inserts on turbulent flow heat exchangers: The overall enhancement ratio criteria," *International Communications in Heat and Mass Transfer*, vol. 55, pp. 53–62, 2014.

[4] Y. Wang, M. Hou, X. Deng, L. Li, C. Huang, H. Huang et al., "Configuration optimization of regularly spaced short-length twisted tape in a circular tube to enhance turbulent heat transfer using CFD modeling," *Applied Thermal Engineering*, vol. 31, pp. 1141–1149, 2021.

[5] M. Tusar, A. Noman, M. Islam, P. Yarlagadda, and B. Salam, "CFD study of heat transfer enhancement and fluid flow characteristics of turbulent flow through tube with twisted tape inserts," *Energy Procedia*, vol. 160, pp. 715–722, 2019.

[6] C. Yu, Y. Cui, H. Zhang, B. Gao, M. Zeng, and L. Han, "Comparative study on turbulent flow characteristics and heat transfer mechanism of a twisted oval tube with different twisted tapes," *International Journal of Thermal Sciences*, vol. 174, p. 107455, 2022.

[7] K. Kim, and K-S. Lee, "Frosting and defrosting characteristics of surface-treated louvered-fin heat exchangers: Effects of fin pitch and experimental conditions," *International Journal of Heat and Mass Transfer*, vol. 60, pp. 505–511, 2013.

[8] A.A.R. Darzi, M. Farhadi, K. Sedighi, R. Shafaghat, and K. Zabihi, "Experimental investigation of turbulent heat transfer and flow characteristics of SiO2/water nanofluid within helically corrugated tubes," *International Communications in Heat and Mass Transfer*, vol. 39, pp. 1425–1434, 2012.

[9] A.H. Yousif, and M.R. Khudhair, "Enhancement heat transfer in a tube fitted with passive technique as twisted tape insert - A comprehensive review," *American Journal of Mechanical Engineering*, vol. 7, no. 1, pp. 20–34, 2019.

[10] S.N. Sarada, "Enhancement of heat transfer using varying width twisted tape inserts," *International Journal of Engineering, Science and Technology*, vol. 2, no. 6, pp. 107–118, 2010.

[11] M.M. Bhuyan, U.K. Deb, M. Shahriar and S. Acherjee, "Simulation of heat transfer in a tubular pipe using different twisted tape inserts," O*pen Journal of Fluid Dynamics*, vol. 7, pp. 397–409, 2017.

[12] S. Bhattacharyya, "Fluid flow and heat transfer in a heat exchanger channel with short-length twisted tape turbulator inserts," *Iranian Journal of Science and Technology, Transactions of Mechanical Engineering*, vol. 44, pp. 217–227, 2020.

[13] B.P. Singh, "A review paper of twisted tape inserts," *International Journal of Applied Engineering Research*, vol. 14, pp. 58–65, 2019.

[14] M.M.K. Bhuiya, M.S.U. Chowdhury, M. Shahabuddin, M. Saha and L.A. Memon, "Thermal characteristics in a heat exchanger tube fitted with triple twisted tape inserts," *International Communications in Heat and Mass Transfer*, vol. 48, pp. 124–132, 2013.

[15] N. Piriyarungrod, S. Eiamsa-ard, C. Thianpong, "Heat transfer enhancement by tapered twisted tape inserts," *Chemical Engineering and Processing: Process Intensification*, vol. 96, pp. 62–71, 2015.

[16] S.A. Dahake, S.C. Pillai, and H.J. Golar, "A review on heat transfer enhancement using various twisted tapes," *International Journal of Engineering Science and Technology*, vol. 6, no. 5, pp. 1–4, 2014.

[17] M.T. Sonawane, M.P. Patil, M.A. Chavhan, and B.M. Dusane, "A review on heat transfer enhancement by passive methods," *International Research Journal of Engineering and Technology*, vol. 3, no. 9, pp. 1567–1574, 2016.

[18] S. Adeyeye, T.J. Ashaolu, and D. Babu, "Food drying: A review," *Agricultural Reviews*, pp. 1–8, 2022.

[19] C.A. Komolafe, A.O.D. Adejumo, O. Awogbemi, and A.D. Adeyeye, "Development of a cocoa beans batch dryer," *American Journal of Engineering Research*, vol. 3, no. 9, pp. 171–176, 2014.

[20] M.A. Waheed, and C.A. Komolafe, "Temperatures dependent drying kinetics of cocoa beans varieties in air-ventilated oven," *Frontiers in Heat and Mass Transfer*, vol. 12, no. 8, pp. 1-7, 2019.

[21] B.F. Dzelagha, N.M. Ngwa, and D. Nde Bup, "A review of cocoa drying technologies and the effect on bean quality parameters," *International Journal of Food Science*, vol. 1, p.8830127, 2020.

[22] M. Ndukwu, A. Ogunlowo, and J. Olukunle, "Cocoa bean (Theobroma cacao L.) drying kinetics," *Chilean Journal of Agricultural Research*, vol. 70, pp. 633–639, 2010.

[23] S.D. Salman, A.A.H. Kadhum, M.S. Takriff and A.B. Mohamad, "CFD simulation of heat transfer and friction factor augmentation in a circular tube fitted with elliptic-cut twisted tape inserts," *Mathematical Problems in Engineering*, vol. 2013, p. 163839, 2013.

[24] F.D. Banboye, M.N. Ngwabie, S.A. Eneighe and D.N. Bup, "Assessment of greenhouse technologies on the drying behavior of cocoa beans," *Food Science & Nutrition*, vol. 8, pp. 2748–2757, 2020.

[25] S.E. Agarry, "Modelling the drying characteristics and kinetics of hot air-drying of unblanched whole red pepper and blanched bitter leaf slices," *Turkish Journal of Agriculture - Food Science and Technology*, vol. 5, no. 1, pp. 24-32, 2017.

[26] A. Al-Hilphy, and A. Alrikabi, "Mathematical modeling and experimental study on thin layer halogen dryer strawberry and study it's effect on antioxidant activity," *American Journal of Agricultural and Biological Sciences*, vol. 8, no. 4, pp. 268–281, 2013.

[27] R. Kumar, M. Malik, and A. Sharma, "Drying kinetics and effects of different drying methods on nutritional quality of raw and differently blanched green peas," *Journal of Current Research in Food Science*, vol. 2, no. 2, pp. 44–56, 2021.

[28] C. Hii, M.C. Law, "Modeling of thin layer drying kinetics of cocoa beans during artificial and natural drying," *Journal of Engineering Science and Technology*, vol. 3, no. 1, pp. 1–10, 2008.

[29] S. Mishra, J.K. Sahu, N. Sanwal, and N. Shama, "Hot air convective drying of small cardamom (Elettaria cardamomum Maton): Evaluation of drying, color, and aroma kinetics," *Journal of Food Process Engineering*, vol. 44, pp. 1-11, 2021.

[30] C. Taveesuvun, S. Tirawanichakul and Y. Tirawanichakul, "Equilibrium moisture content modeling and study of circulating-bed drying kinetics of non-fragrant and fragrant paddy varieties," *Trends in Sciences*, vol. 19, no. 14, pp. 1-12, 2022.

[31] A.I. Gbasouzor, J.E. Dara, and C.O. Mgbemena, "Statistical prediction of the drying behavior of blanched ginger rhizomes," *Journal of Advances in Science and Engineering*, vol. 4, pp. 98–107, 2021.

[32] P. Praneetpolkrang, and K. Sathapornprasath, "Thin-layer drying model of jackfruit using artificial neural network in a far infrared dryer," *Engineering and Applied Science Research*, vol. 48, pp. 181–189, 2021.

[33] V. Thi, B. Nusantoro, R. Aidoo, P.H. Anh, H.T. Toan, K. Messens and K. Dewettinck, "Physico-chemical properties of fourteen popular cocoa bean varieties in Dongnai – highland Vietnam," *Can Tho University Journal of Science*, vol. 4, pp. 81–86, 2016.

[34] P. Guda, S. Gadhe, and S. Jakkula, "Drying of cocoa beans by using different techniques," *International Journal of Agriculture Innovations and Research*, vol. 5, no. 5, vol. 23, pp. 859-865, 2017.

[35] E. Erdiwansyah, Mahidin, H. Husin, Nasaruddin, Muhtadin, M. Faisal, "Combustion efficiency in a fluidized-bed combustor with a modified perforated plate for air distribution," *Processes*, vol. 9, pp. 1-12, 2021.

[36] T. Gebreegziabher, A. Oyedun, and D. Hui, "Optimum biomass drying for combustion – A modeling approach," *Energy*, vol. 53, pp. 67–73, 2013.

[37] V. Deus, M. Silva, L. Maciel, L.C.R. Mianda, E.Y. Hirooka, S.E. Soares et al. "Influence of drying methods on cocoa (Theobroma cacao L.): Antioxidant activity and presence of ochratoxin A," *Food Science and Technology*, vol. 38, pp. 278-285, 2018.

[38] U. Inyang, I. Oboh, and B.R. Etuk, "Kinetic models for drying techniques-food materials," *Advances in Chemical Engineering and Science*, vol. 8, pp. 27–48, 2018.

[39] G. Austin Ikechukwu, and S. Omenyi, "Statistical determination of the drying characteristics of thin layer ginger rhizomes," *Journal of Advances in Science and Engineering*, vol. 4, pp. 98–107, 2021.

[40] C. Hii, C. Law, M. Cloke, "Improving Malaysian cocoa quality through the use of dehumidified air under mild drying conditions," *Journal of the Science of Food and Agriculture*, vol. 91, no. 2, pp. 39–46, 2011.